Available online at www.sciencedirect.com
SCIENCE DIRECT®
Journal of Molecular Catalysis A: Chemical 228 (2005) 255–266
JOURNAL OF MOLECULAR CATALYSIS A: CHEMICAL
www.elsevier.com/locate/molcata

One-step generation of highly selective hydrogenation catalysts involving sub-nanometric Cu_2O supported on mesoporous alumina: strategies to control their size and dispersion

Sabine Valange[a,*], Annie Derouault[a], Joël Barrault[a], Zelimir Gabelica[b]

[a] *LACCO, UMR CNRS 6503, ESIP, 40 Av. Recteur Pineau, F-86022 Poitiers, France*
[b] *Université de Haute Alsace, ENSCMu, GSEC, 3 rue A. Werner, F-68093 Mulhouse, France*

Available online 5 November 2004

Abstract

A series of binary Cu–Al surfactant-assisted mesoporous precursors have been prepared through direct synthesis and catalytically evaluated in the selective hydrogenation of conjugated α,β-unsaturated aldehyde (cinnamaldehyde) to the corresponding unsaturated alcohol in the liquid phase. The resulting material consists in a mesoporous alumina substrate involving a ripple sheet type-texture onto which "Cu hydroxynitrate" domains of uniform size were dispersed. After calcination, these particles yield sub-nanometer (<1 nm) and larger (20–40 nm) CuO particles. An original model implying a homogeneous temperature-induced particle accretion is proposed to explain this bimodal dispersion. A specific re-evaluation of some synthesis parameters allowed us to optimize the relative size, dispersion and final stabilization of these particles. Upon reduction, CuO yields sub-nanometric Cu_2O and metallic Cu particles of relatively uniform size. The remarkable selectivity (70%) of the binary mesoporous samples towards the hydrogenation of the carbonyl group of cinnamaldehyde is due to the presence of Cu_2O particles that are probably in relatively strong interaction with the alumina pore walls. By contrast, solids involving Cu nitrate impregnates on either mesoporous and commercial (bulky) γ-alumina performed poorly towards the formation of cinnamyl alcohol, arguing for a fundamental difference in the electronic states of the various supported Cu particles with respect to those generated on samples by direct synthesis.

Keywords: Mesoporous alumina; Binary CuO–Al_2O_3 mesoporous phases; Dispersed copper particles; Sub-nanometric Cu_2O particles; Strong copper–alumina interaction; Cinnamaldehyde hydrogenation

1. Introduction

Copper-based catalysts are very efficient for many catalytic reactions, such as nitrogen oxide removal, for various fine chemicals conversions (selective hydrogenation, oxidation, amination, etc.) [1], and for the oxidation of organic compounds in liquid phase [2]. Because the overall performance of such catalysts depends on the nature and structure of the copper phase and the supporting oxide, the promotion of a strong interaction between both species is particularly required to limit deactivation and leaching of copper during the reaction. In fact, it has been shown that alumina, possibly along with a promotor, plays an interesting structural role, probably through minimizing the sintering of the Cu oxidic or metallic phases [3,4].

From a fundamental point of view, the selective hydrogenation of (conjugated or not) α,β-unsaturated aldehydes to the corresponding allyl alcohols is considered as an important problem of chemio- and regioselectivity, for which performant and very selective catalysts are of great demand. α,β-unsaturated carbonyl compounds can be transformed into saturated aldehydes by hydrogenating the C=C bond or preferentially into unsaturated alcohols through the selective hydrogenation of C=O bonds. Both products undergo subsequent hydrogenation to yield the corresponding saturated alcohols, possibly also some unwanted products through hydrogenolysis or decarbonylation [5,6]. As the hydrogenation of an unsaturated carbonyl compound generally produces a saturated carbonyl compound (ΔH

* Corresponding author. Tel.: +33 5 49 45 40 48; fax: +33 5 49 45 33 49.
E-mail address: sabine.valange@univ-poitiers.fr (S. Valange).

1381-1169/$ – see front matter © 2004 Elsevier B.V. All rights reserved.
doi:10.1016/j.molcata.2004.09.034

[(C=C) → (C–C)] = −120 kJ mol^{-1} and ΔH [(C=O) → (C–OH)] = −50 kJ mol^{-1}), an important challenge is to obtain the unsaturated alcohol with high selectivity.

Such reactions are currently catalyzed by systems involving supported noble metals, such as Pt, Pd, Ru [7,8]. However, noble metals have been found to predominantly hydrogenate the C=C bond rather than the C=O group [9], though the selectivity towards unsaturated alcohols could be improved by adding promotors such as Fe or Sn [10–12].

The use of non-noble metals (Cu. . .) for selectively hydrogenating α,β-unsaturated aldehydes, by preferentially saturating the carbonyl group when it is not adjacent to the C=C bond, has also been reported in literature [13]. For example, attempts for improving the intrinsic catalytic properties of Cu-supported SiO_2 include the use of promoters such as V_2O_5 or Pd [14]. The resulting catalysts proved more efficient in selectively hydrogenating the carbonyl group of cinnamaldehyde to yield the corresponding cinnamyl alcohol. The selectivity of such phases was either attributed to a good dispersion of the copper particles on the silica support, or to a stronger Cu^0 (or Cu_2O)-support interaction, enhanced by the presence of promoters.

As part of an extensive effort to conceive catalysts involving a strong metal-support interaction favoring the hydrogenation of the C=O bond of α,β-unsaturated aldehydes, binary (Cu–Al), ternary (Cu–Zn–Al) or quaternary (Cu–Ni–Zn–Al) catalysts obtained by co-precipitation have been recently evaluated [15,16]. Cinnamaldehyde hydrogenation on binary Cu–Al samples proceeded via a monofunctional pathway on metallic copper that favors hydrogenation of the C=C bond forming predominantly the unsaturated aldehyde [16]. Increasing the Cu dispersion enhances the cinnamaldehyde conversion rate, but does not modify significantly the selectivity towards the unsaturated alcohol. Ternary and quaternary catalysts were shown to be more active than their binary counterparts, but despite the presence of very small Cu^0 particles highly dispersed in a zinc aluminate spinel phase, the unsaturated alcohol selectivity did not exceed 52.9% at 30% conversion [16]. The formation of this latter compound was attributed to a close interaction between Cu^0 particles and Zn^{2+} active sites via a dual-site reaction pathway.

All these examples comfort the idea that the catalyst preparation is a critical factor for improving the dispersion of a thermostable active phase, along with the selection of an appropriate substrate, preferentially exhibiting a high surface area, like the organized mesoporous oxides.

In an attempt to improve the catalytic performances of copper-supported alumina systems that are currently prepared by conventional impregnation or exchange procedures, we have recently described a new route to prepare high surface mesoporous alumina [17], but also binary $CuO–Al_2O_3$ and ternary $CuO–ZnO–Al_2O_3$ mixed mesoporous phases [18,19], where the metallic oxide and the support are simultaneously generated through direct synthesis. The originality of our approach consisted in synthesizing mesostructured metalloaluminate precursors exclusively composed of Cu, (Zn) and Al oxidic species. Syntheses were performed in aqueous media at ambient temperature through a careful pH control that predominantly adjusts the final positive charge of both cationic aluminum hydroxydic and copper hydroxynitrate species, for their further optimal interaction with the negatively charged surfactant molecules (fatty acids or their salts). Preliminary results indicated that these systems behaved as excellent catalysts in selective hydrogenation of conjugated α,β-unsaturated carbonyl compounds (cinnamaldehyde) to their corresponding unsaturated alcohols (cinnamyl alcohol referred here as CNOL) [20].

Here, we report a more in depth study of the influence of some key synthesis parameters of our recipe, aiming at generating and better stabilizing, after controlled calcination and further reduction, reduced copper species involving the following optimized characteristics: a very small and uniform size, a quasi homogeneous dispersion and a strong interaction with the mesoporous alumina substrate. The main synthesis variables investigated here are the order of addition of the reactants and the final pH of the medium, parameters that are thought to readily favor, after reduction, a strong metal-support interaction without affecting the overall mesoporosity of the resulting binary phase. The other goal of this approach consists in determining the size and dispersion of the Cu active phase, in evaluating the strength of the $Cu–Al_2O_3$ interaction and in comparing the catalytic performances (activity and selectivity towards the unsaturated alcohol) of the mesoporous Cu–Al phases with those of their compositional analogs prepared through a classical impregnation of a (bulky) γ-alumina and a mesoporous alumina, by Cu^{2+} nitrate.

2. Experimental

2.1. Sample preparation

The general synthesis procedure adopted for the straightforward preparation of binary mesoporous phases involves the use of a solution of aluminum polymeric species (Keggin polycations $[AlO_4Al_{12}(OH)_{24}(H_2O)_{12}]^{7+}$ "Al_{13}") and copper nitrate, along with a solution of mixed anionic (sodium palmitate) and cationic (cetyltrimethylammonium bromide) surfactants, so as to achieve a globally anionic surfactant medium. As described elsewhere [18], all syntheses were conducted at ambient temperature with a careful pH control during the simultaneous addition of the reactants, until the formation of blue colored solids and colorless mother liquors. The resulting suspension was maintained under stirring for at least 15 h. The solid was recovered by filtration, washed with deionized water and dried at 80 °C in an oven overnight. The preferred initial pH of the synthesis batch was shown to be 6.5 in our previous contribution [18] and it appeared to be critical to maintain during the synthesis course for a steady stabilization of the resulting rippled sheet Al-based mesostructure.

Two other Cu–Al mesoporous phases were also prepared at pH = 6.1. They only differ by the order of addition of the reactants (simultaneous or successive addition of the mixture of surfactants and of the basic solution in the inorganic precursors solution). The selected Cu amount in all the binary samples in this work was 15 mol%, thus 15 mol Cu/100 mol (Cu + Al).

Two binary impregnated Cu–Al catalysts involving the same final copper content, were also prepared for comparison through a classical wet impregnation of a commercial γ-alumina (GFSC Rhône Poulenc, 200 $m^2\ g^{-1}$) or of an organized mesoporous alumina [17], with an aqueous solution of copper(II) nitrate. After impregnation, all solids were dried overnight at 120 °C in an oven and calcined under nitrogen flow at 500 °C at a heating rate of 1 °C min^{-1}, then maintained isothermally under flowing air at the same temperature for 7 h.

2.2. Catalyst characterization

All as-synthesized and calcined (N_2 then air at 500 °C) samples were characterized by powder X-ray diffraction using a Bruker D5005 diffractometer with monochromatized Cu Kα radiation (40 kV, 30 mA). The spectra were scanned with a rate of 0.04° s^{-1} and with a step size of 2 s from 1° to 10° 2θ in order to verify that all the calcined solids still show mesoporous characteristics after elimination of the surfactant molecules.

Bulk chemical analysis for C, H, N, Al and Cu was achieved by atomic absorption. The surface area and pore size analysis was carried out by adsorption–desorption of nitrogen on a Micromeritics ASAP 2010 instrument (−196 °C). Prior to N_2 adsorption, the samples were degassed under vacuum at 90 °C for 1 h followed by a further heating at 300 °C for a few hours. The BET surface areas were evaluated from the linear part of the BET plots and the pore volume and average pore diameter of the catalysts were determined by the BJH method from the adsorption branch [21].

The surface of all the binary mesoporous $CuO–Al_2O_3$ phases and of their impregnated counterparts, as well as the Cu particle size analysis were investigated by TEM (Philips CM120 microscope) coupled to an EDX spectrometer (fixed probe). Electron microdiffraction patterns were also recorded to identify the nature of the copper-bearing particles. The samples were at first included in a resin that was cut into sections of 30–50 nm with a microtome equipped with a diamond cutter, before they were supported on a carbon-coated gold grid.

Temperature programmed reduction (TPR) experiments of the Cu oxidic particles generated upon controlled calcination of the binary Cu–Al as-synthesized phases were performed by using pulsed chromatography at 550 °C, while hydrogen pulses (in argon flow) were regularly injected. A heating rate of 4 °C min^{-1} and about 30 mg of sample were selected to enhance resolution and avoid hot spots. Prior to experiment, the samples were activated in argon flow up to a maximum temperature of 500 °C, for 2 h. Since water is formed during reduction, a dessicant is inserted at the exit of the reactor, before the gasses enter the thermal conductivity detector.

2.3. Selective cinnamaldehyde hydrogenation

The calcined samples were first reduced under hydrogen flow at 350 °C for 8 h at a heating rate of 4 °C min^{-1}. The catalytic hydrogenation of cinnamaldehyde (CNA) was carried out at atmospheric pressure at 160 °C in a batch reactor. The solution involved about 0.2 g of catalyst dispersed in 25 mL of propylene carbonate as solvent and 1 mL of CNA. The liquid phase was first purged by hydrogen at room temperature by stirring for 20 min to remove traces of air and dissolved oxygen in the medium, before introducing the catalyst. The liquid phase was then continuously swept by a hydrogen flow of (1 L h^{-1}) under vigorous stirring.

The analysis of the reaction products was performed on a Varian 3900 gas chromatograph (GC) equipped with a flame ionization detector (FID) and a capillary Chrompack CP Sil-8 CB column (length 25 m, 0.53 mm i.d., film thickness 2 μm) with flowing N_2 as carrier gas. The products were calibrated by using pure compounds (ACROS, purity > 98%, except for CNA > 99%), i.e. cinnamaldehyde, cinnamly alcohol, hydrocinnamaldehyde (3-phenylpropionaldehyde) and 3-phenyl propanol (3-phenylpropyl alcohol) diluted in a propylene carbonate solution. The conversion of cinnamaldehyde and product distribution were followed as a function of time on stream by gas chromatography of microsamples periodically withdrawn and centrifuged before analysis. For all the samples, the cinnamyl alcohol (CNOL) selectivities were compared at the same cinnamaldehyde conversion, typically 50%.

3. Results and discussion

3.1. Structural and porous characteristics of the samples

We have shown in a previous contribution that pure mesoporous alumina [17] and Al-rich [(Cu) ≤ 10%] binary mesophases [18] prepared under comparable conditions exhibit a periodic arrangement with at least three diffraction peaks and with XRD d_{100} values close to 5.5 nm, provided the pH of the synthesis batch was close to 6.5. High mesoporous volumes and surface areas, as well as narrow pore size distributions indicate a regular mesostructure of good quality, although the long range order was not as high as for siliceous mesoporous materials. Indeed aluminum oxidic species undergo a too fast precipitation in aqueous media preventing the formation of a perfectly hexagonal structure after interaction with appropriate surfactant molecules [17]. Nevertheless, the overall shape of the N_2 isotherm with a weak hysteresis loop (not shown) confirms the regularity of the mesopores in the Al phase [17]. Upon increasing the Cu loading

Table 1
Pore characteristics of selected binary (Cu-Al) mesoporous samples

Sample (precursor)	pH and addition of NaOH	S_{BET} ($m^2\ g^1$)	V_p ($cm^3\ g^1$)	$Ø_p$[a] (nm)
1. CuAl meso	6.5 – Simultaneous	355	0.54	4.0
2. CuAl meso	6.1 – Added afterwards	350	0.38	3.6

[a] Pore diameter: determined from the adsorption branch.

(Cu ≥ 15%), the organization of the alumina substrate starts to change, as suggested by the loss of the third XRD peak. Nevertheless, the residual calcined Cu–Al phase synthesized upon simultaneous addition of all the reactants (sample 1, Table 1), exhibits an adsorption–desorption isotherm with a marked hysteresis (Fig. 1) typical of mesostructured solids. In addition, the adsorption step occurs at a higher p/p_0 value, which is related to a wider pore size distribution compared to pure mesoporous alumina or to mixed (Cu–Al) phases involving low Cu contents. Sample 1 exhibits a surface area of $355\ m^2\ g^{-1}$, and a pore diameter of 4 nm. The loss of surface area coupled to the increase in pore diameter with respect to the binary sample involving 5% Cu ($552\ m^2\ g^{-1}$ and 2.9 nm) [19] confirms that Cu^{2+}-enriched phases start to de-organize the regular structure of the mesoporous alumina substrate.

Sample 2 (Table 1) was prepared at a slightly lower pH (6.1) than sample 1 (pH = 6.5) and under slightly different synthesis conditions. NaOH was not added simultaneously with the surfactant mixture to the solution containing the inorganic Cu and Al precursors, but after the former solution was added. This sample exhibits a less pronounced hysteresis loop than sample 1 that occurs at a lower p/p_0 value (Fig. 1), thus corresponding to a narrower pore size distribution. Data from Table 1 (comparable surface areas and pore diameters with slightly different pore volumes of samples 1 and 2) suggest that the influence of the addition order of the reactants and probably also the pH seem to induce little changes in the intrinsic organization of the resulting mixed (Cu–Al) mesoporous phases, except in terms of the total pore volume. In addition, both phases are stable to at least 500 °C and retain their porosity as ascertained by the presence of an intense broad XRD peak in the mesoporous range (1–10 ° 2θ).

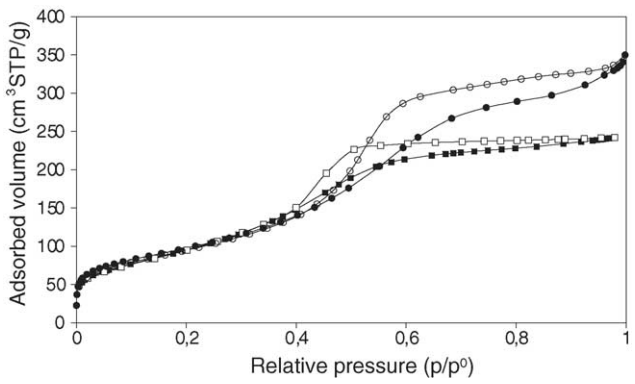

Fig. 1. Nitrogen adsorption–desorption isotherms of two selected binary ($CuO–Al_2O_3$) mesoporous samples calcined under N_2 then in air at 500 °C: (■) sample 1, (●) sample 2 (Table 1). Filled and blank characters refer to the adsorption and desorption steps, respectively.

3.2. Cu dispersion in the mesoporous and impregnated Cu–Al phases

The various copper-bearing species in the as-synthesized and calcined Cu–Al phases were identified by combined TEM-EDX analyses (Table 2).

The chemical composition of sample 1, as derived from combined bulk and thermal analyses, is the following: $[Cu_{14.3}\ Al_{75}\ (OH)_{222}\ (NO_3^-)_{12}\ (H_2O)_{41}]\ [(C_{16}H_{31}OO^-)_{26.7}\ (CTMA^+)_{6.7}]$. More particularly, the quantitative incorporation of both copper and surfactant molecules shows the advantage of a careful pH-monitored and surfactant-assisted precipitation in aqueous solution. In contrast to the case of pure mesoporous alumina where no nitrate ions were found involved in the wall structure [17], the excess of nitrogen determined in all the binary mesoporous phases indicates that nitrates ions are incorporated in the as-synthesized compounds, probably as charge compensating anions linked to Cu^{2+} species. Indeed, as shown by Wells [22], Cu^{2+} salts readily precipitate upon progressive pH increase, to form a variety of basic salts, for example hydroxynitrates, like e.g. $Cu_2(OH)_3NO_3$ (mineral gerhardite), where $Cu_2(OH)_3O$ polymeric sheets are interlinked through nitrate ions that are hydrogen-bonded to the OH^- ions of the adjacent layers. It is therefore expected that in the selected pH range of 6–7, similar pre-polycondensed Cu basic nitrates would also form along with the Al hydroxy-oxy species that are structured in the presence of surfactant micelles. Such Cu hydroxynitrate domains that do not necessarily involve a specific stoichiometry (Cu/OH/NO_3 ratio) are consequently accommo-

Table 2
Particle size determined by TEM in the various as-synthesized and calcined binary (Cu-Al) mesoporous samples

Sample (precursor)	Particle size (nm)	
	CuHN[a] in precursor	CuO in calcined (mean Ø)
1. Cu-Al meso (pH = 6.5, simultaneous)	1–2	<1 and 30–35
2. Cu-Al meso (pH = 6.1, adjustment)	1	<1 and 60
3. Cu-Al meso (pH = 6.1, simultaneous)	NI	<1 and 25
4. $Cu_{impregnation}/Al_2O_3$ mesoporous	–	<1
5. $Cu_{impregnation}$/bulky γ-Al_2O_3	–	20–30 and >1000

NI: not investigated.
[a] CuHN = Cu^{2+} hydroxynitrate.

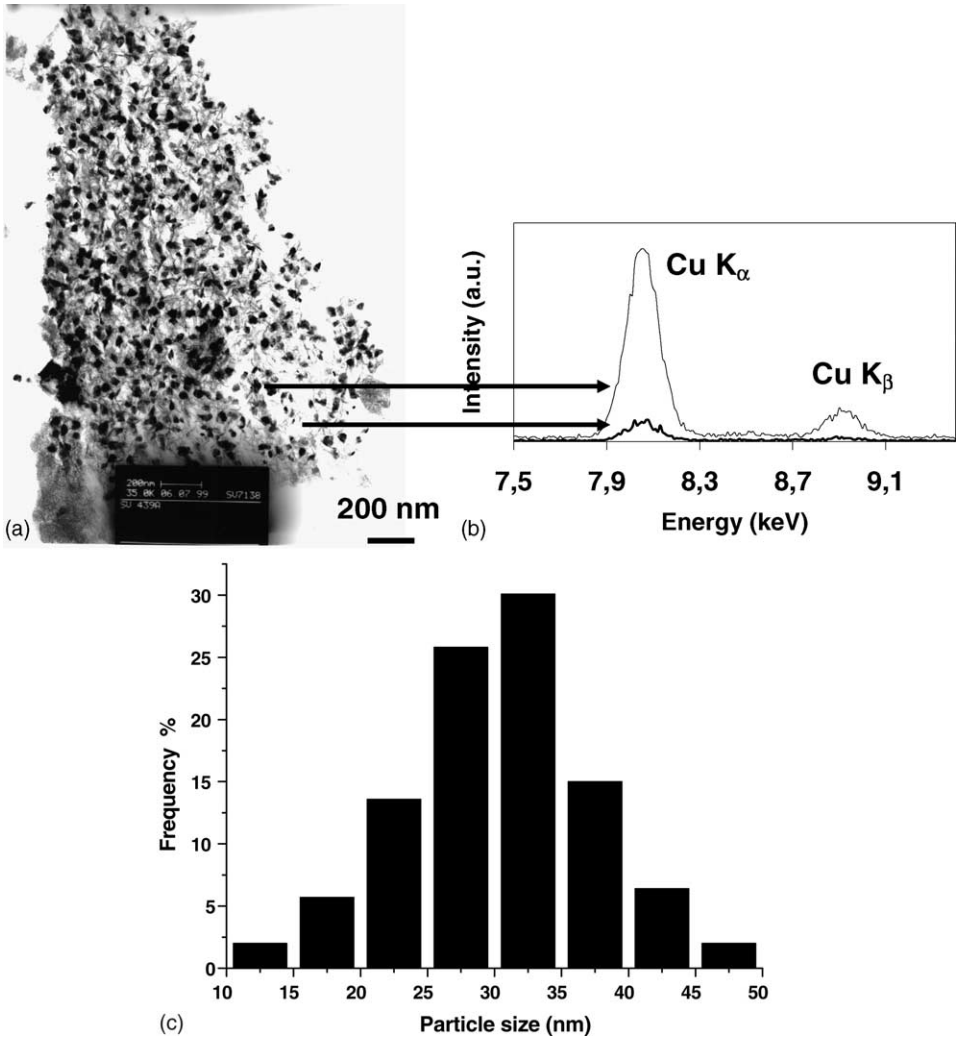

Fig. 2. (a) TEM image of a CuO–Al_2O_3 mesoporous phase calcined under N_2 then in air at 500 °C (sample 1), (b) EDX analysis of various areas of the same sample. Regular curve: analysis of the 35 nm nanometer sized CuO particle; bold curve: probing of the clear parts of the micrograph where sub-nanometric CuO particles are not visible and (c) statistical particle size (diameter) distribution measured for 140 particles on TEM image 2a for sample 1.

dated within the alumina mesophase to eventually form the mixed binary phase.

TEM analysis of as-synthesized sample 1 reveals that the alumina mesophase is regularly studded with a large number of very small Cu-bearing islets of about 1 or 2 nm in diameter, bringing more evidence for the existence of the very small Cu hydroxynitrates (CuHN) particles. This homogeneous dispersion is obviously inherent to our synthesis procedure that involves the simultaneous precipitation of the Cu and Al species in the presence of surfactants and their further structuring into a mesoporous solid at a correctly selected pH value. Upon calcination, both TEM and EDX probing of the dark spots dispersed within the mesostructured Al-rich sheets, confirm the presence of Cu-bearing particles of about 30–35 nm in diameter (Fig. 2a and b, Table 2). The size distribution is illustrated in the corresponding histogram (Fig. 2c). Spot electron microdiffraction identified the presence of monoclinic CuO (figure not shown but similar to Fig. 3b, see below).

Surprisingly, the presence of another population of very small nanometer sized CuO particles were also detected by spot EDX probing the clear parts of the surface seen on the micrograph (Fig. 2a and b). The fact that these particles could not be visualized as dark spots under our experimental conditions (microscope resolution limited to about 1 nm), suggests their sub-nanometric size and, as a consequence, their regular dispersion onto the substrate surface. The fact that the larger CuO particles are also regularly dispersed and keep their size relatively uniform, suggests that they are also moderately to strongly interacting through oxygens with the mesoporous alumina sheets and that their significant interaction prevents their possible further clustering upon heating.

The regular dispersion and relative uniformity of sizes of the copper species in this sample was explained by a mechanism [19] involving a homogeneous accretion (agglomeration) of very small Cu particles to larger ones after the thermal treatment (used to eliminate the surfactant molecules occluded in the mesophase). The final result of the accretion

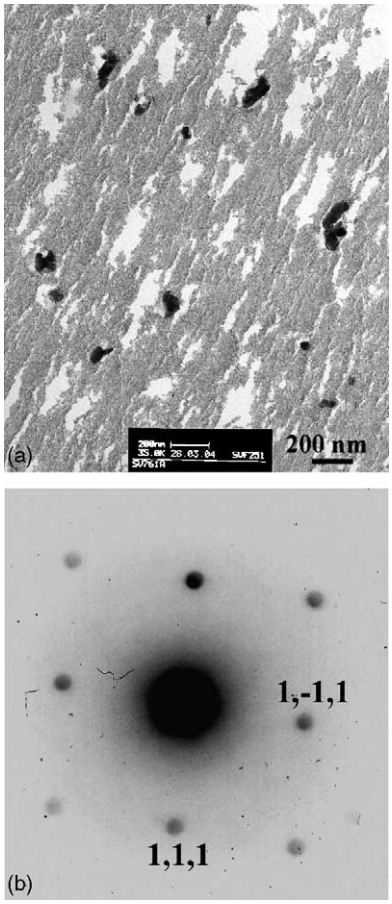

Fig. 3. TEM image (a) and electron microdiffraction pattern of the dark spots (b) in calcined CuO–Al_2O_3 mesoporous phase (sample 2, Table 2).

phenomenon would consist in the decrease of the size of the small 1–2 nm Cu hydroxynitrate islets (that are progressively decomposed to CuO while still fairly strongly retained onto the substrate surface). Indeed, the scraping away of the outer (CuO) crust from the "bigger" particles (1–2 nm CuHN that soon become CuO) and its further creeping towards a restricted number of these initial islets that, for some reason, act as a "sink", results in a substantial increase of the size of these sinks (that eventually form larger CuO clusters of about 30–35 nm through a progressive accumulation of CuO on their surface), while the bottom of the residual scraped particles would remain strongly attached to the surface and therefore remain highly dispersed as well. The fact that all the sub-nanometer sized CuO particles stay well dispersed even at 500 °C, accounts for their relatively strong initial interaction with the mesoporous alumina substrate.

Upon reduction, a double Cu particle population (<1 nm and about 35 nm) is still observed (histogram similar to that than for CuO in Fig. 2c, not shown here).

Considerable changes occurred upon slightly modifying the synthesis procedure of the binary Cu–Al mesophase. For sample 2, NaOH solution (used to impose the final pH) was added after mixing the surfactants and the (Cu, Al) inorganic solution and this systematically yielded a final pH of 6.1. Oppositely to sample 1 (reactants added simultaneously and final pH of 6.5), calcined sample 2 exhibited larger and more randomly dispersed Cu domains as detected by TEM (Fig. 3a). Electronic microdiffraction analysis showed that these large dark spots (about 60 nm in size) are composed of monoclinic copper oxide (Fig. 3b). Their accurate size evaluation through building histograms could not be achieved because of their agglomeration. Their relatively large size and more random dispersion (Fig. 3a) probably reflect the less efficiently controlled precipitation of CuHN type particles upon local pH variations during the final NaOH addition. The small (sub)-nanometer sized CuO particles were still present, as substantiated by EDX probing the clear parts of the micrograph.

Because the amount of incorporated Cu in each sample is the same (quantitative incorporation), the fact that we observed a significantly lower amount of slightly larger CuO clusters (compared to sample 1), means that the resulting sub-nanometer CuO content has considerably increased in sample 2. Following the accretion model, this also suggests that the total number of CuHN islands (precursors to sub-nanometric CuO in the calcined samples) is larger in the as-made sample 2 than in sample 1, because, according to the model [19], every single CuHN particle should also yield one sub-nanometric CuO particle after scraping away of the outer CuO "crust" from its surface. In other words, for the same global Cu content, if sample 2 (precursor) involves a larger amount of CuHN islands (than sample 1), these islands should necessarily have a smaller size. This is confirmed by the (rough) TEM evaluation (Table 2). The fact that the number of large CuO clusters had decreased in the calcined sample (TEM) implies that the remaining number of "residual" sub-nanometric CuO particles should necessarily be larger than in sample 1 because the total amount of superficial Cu available for a steady accretion is also necessarily smaller. Unfortunately, we did not dispose of any appropriate technique able to count sub-nanometric particles to ascertain this conclusion.

This scheme also allows us to speculate that the strength of the interaction of sub-nanometric CuO with the alumina surface could be similar in both samples. However, the accretion model does not indicate whether the size of the final particles is necessarily directly related to the strength of their interaction with the support. For a given particle size and dispersion, such interaction could be qualitatively evaluated by TPR (see below).

The above observations show how a slight variation in the final pH, but also its local variation during the NaOH addition, could markedly influence the "nucleation" of the resulting CuHN islands (thus their number and size) that readily integrate the alumina surface.

Sample 3 was prepared at pH 6.1 but using a different order in mixing the reactants, namely simultaneous addition of the solutions as in sample 1, to avoid local pH variations. TEM micrograph of calcined sample 3 evidenced a high and still rather homogeneous dispersion of spheroidal CuO particles onto the surface of the mesoporous alumina (Fig. 4a

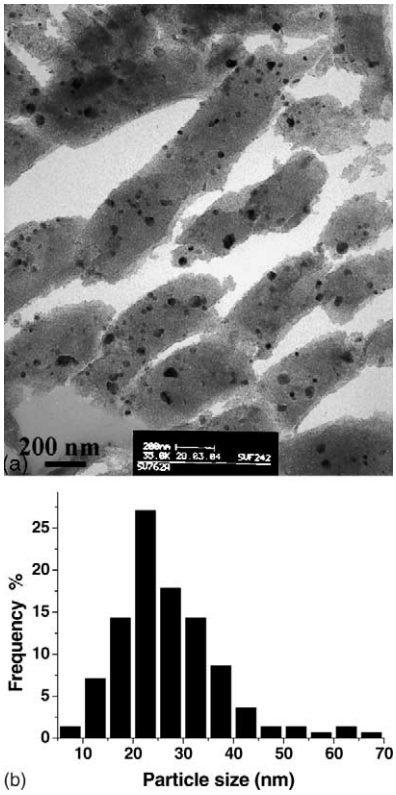

Fig. 4. (a) TEM image of calcined CuO–Al_2O_3 mesoporous phase (sample 3, Table 2) and (b) statistical particle size (diameter) distribution measured for 140 particles on this TEM image.

and Table 2), with a mean particle size of about 25 nm (histogram shown in Fig. 4b). Although a close analysis of the micrograph also showed some smaller (about 10–15 nm) and a few larger CuO clusters, extending up to 70 nm (Fig. 4b), the CuO particles in sample 3 are definitely more homogeneous in size than in sample 2. For sample 3, while combined TEM-EDX data logically confirmed the presence of very small CuO islets, their number is probably also larger than in sample 1 and comparable to sample 2, as suggested by the decreased amount of the larger 25 nm sized CuO particles (with respect to sample 1). This important experiment confirms that it is the pH and not the order of addition of the reactants that plays a major role in tailoring the size of the CuHN islands in the precursor phases and, hence, the size of the final CuO particles (of both populations) in the calcined counterparts. In other words, an adequate adjustment of the final pH is required to modulate, in the binary mesoporous samples, the relative amounts of both sub-nanometric and larger CuO particles, along with their degree of dispersion, in order to predominantly favor those particles required for a specific catalysis.

The dispersion of copper in samples prepared by classical wet impregnation of two different alumina supports was also investigated by TEM-EDX analyses (samples 4 and 5, Table 2). Sample 4 was obtained after impregnation with copper nitrate of an organized mesoporous alumina phase prepared following our original recipe [17], while sample 5 was achieved by a similar impregnation of a commercial γ-alumina.

Surprisingly, the surface of the Cu-impregnated mesoporous alumina compound, after calcination, appeared to be completely free from any visible (large) CuO domains (TEM not reported). In contrast, EDX analysis coupled to X-ray emission mapping revealed an extremely homogeneous dispersion of very small (TEM-silent) Cu-bearing spots over the surface of the mesoporous alumina support. It seems inappropriate to explain this unexpected uniform particle dispersion by the formation of a relatively strong Cu-support interaction, at least in the impregnated sample 4. One could instead attribute this phenomenon to the high surface area exhibited by the mesoporous alumina ($\sim 450\,m^2\,g^{-1}$) that favors a very good dispersion (but not necessarily a strong retention) of the metallic salt before calcination. For example, it can be assumed that the organized alumina support involves many specific sites of anchoring, probably more numerous and at least different than those occurring on a classical γ-Al_2O_3. Another more probable reason for a good and homogeneous dispersion of such particles could stem from the nature of the copper species itself. Indeed, impregnation under our conditions probably brings (non-hydrolyzed) Cu(II) nitrate species to be dispersed onto the alumina surface. Such a situation is different than the direct synthesis conditions where layered CuHN type phases are generated. Although these latter are probably more bulky than the Cu nitrate species, it has been shown [20] that they readily interact with Al_{13} Keggin polycations prior to (or during) their interaction with the surfactants to form the mixed phase onto which they would disperse as independent islands.

It could appear surprising that the tiny particles in sample 4, probably at the best moderately retained on the alumina surface, do not agglomerate during the oxidative heating. An accretion type model is also less likely to have occurred, as such phenomenon would have resulted in a quite homogeneous dispersion of some new larger CuO clusters visible in TEM, as seen in samples 1–3. Moreover, this model also implies a relatively strong retention of the initial Cu precursors, which is probably not the case here. The absence of any Cu-bearing large particle (TEM), and the deep green color of the residue rather suggest that Cu nitrate species, initially very well dispersed, start to react with the alumina surface during heating so as to yield, at 500 °C, a spinel-like phase (for example $CuAl_2O_4$) where the Cu^{2+} ions stay atomically dispersed. The initial excellent dispersion of the Cu precursor islets and the large alumina surface would favor such solid state reaction like, e.g. $CuO + Al_2O_3 \rightarrow CuAl_2O_4$, at a more moderate temperature than required for a similar reaction in the bulk state, as earlier suggested [23]. In our case, a spinel-like phase could not be detected by XRD because of the too small thickness of the mesoporous walls.

Oppositely, the Cu dispersion on the surface of commercial γ-alumina is particularly heterogeneous. In the calcined sample, TEM analysis reveals the presence of very large CuO

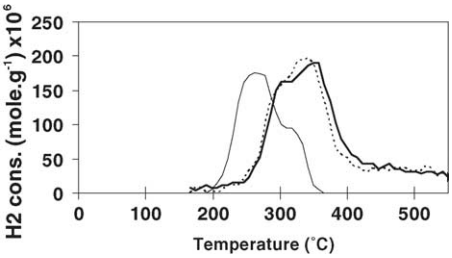

Fig. 5. TPR profiles of calcined binary CuO-Al_2O_3 mesoporous samples (Table 3). Influence of the synthesis procedure: sample 1 (full curve), sample 2 (dotted curve), sample 3 (bold curve).

domains of different sizes (Table 2). Along with the 20–30 nm sized CuO particles, very large aggregates (> 1000 nm) are also present, thereby confirming that this classical alumina neither involves appropriate sites for a good distribution of the active phase, nor has a surface large enough to allow a good dispersion of the Cu-bearing precursor.

3.3. Reducibility and surface properties

TPR data of all the binary CuO–Al_2O_3 mesoporous phases (samples 1–3, Fig. 5 and Table 3) definitively confirm the existence of a dual population of large and sub-nanometer sized particles. The TPR profile of sample 1 shows a two-step reduction. The main TPR peak occurs at about 260 °C, illustrating the reduction of the regular 30–35 nm CuO clusters, while the second peak at about 320 °C could be attributed to the reduction of the very small quasi atomically dispersed CuO particles that are generated through scraping away of the initial CuHN domains following the earlier proposed accretion model [19]. The mean oxidation state of copper derived from hydrogen consumptions is 0.73. A more accurate evaluation of the copper oxidation state during each reduction step, after deconvolution of the two TPR peaks, indicates that CuO (large particles) is totally reduced to Cu^0 (peak at 262 °C), while the oxidation state of copper after the second reduction step, is close to +1, therefore suggesting a reduction of the small CuO particles to Cu_2O particles of the same size [19]. The Cu oxidation state of +1 suggests an overall difficult reduction of the sub-nanometric CuO particles, thereby comforting the hypothesis of their relatively strong interaction with the mesoporous alumina matrix in the reduced sample. However, this does not give any direct indication about the strength of the interaction of their precursors CuO with the same support during the preliminary oxidative calcination process. Nevertheless, the temperature (about 320 °C) corresponding to the reduction of such particles probably better reflects the strength of their retention onto the support than their dispersion and small size. It is probably the reduced Cu_2O that is actually the only strongly retained species and not necessarily their sub-nanometric CuO precursors. Actually the fact that the excellent dispersion of such small particles is maintained at 500 °C argues for their relatively strong retention on the surface while, for catalysis, only their small size and high dispersion (and not necessarily their strong anchoring on the support surface) are needed for such Cu_2O particles to be very selective in the specific reduction of the aldehyde group into the corresponding alcohol (see below).

Table 3
TPR characteristics of the various Cu-Al mesoporous and impregnated samples

Sample (precursor)	T_{max} (°C) (TPR)[a]
1. Cu-Al meso (pH = 6.5, simultaneous)	262 s, 318 m, sh, br
2. Cu-Al meso (pH = 6.1, adjustment)	310 m, sh, 342 s, br
3. Cu-Al meso (pH = 6.1, simultaneous)	310 m, sh, 358 s, br
4. $Cu_{impregnation}/Al_2O_3$ mesoporous	334 s
5. $Cu_{impregnation}/Al_2O_3$ commercial	230 m, 358 s, br

[a] s = strong; m = medium; w = weak; br = broad; sh = shoulder.

By contrast, when the binary CuO–Al_2O_3 mesoporous phase is synthesized at lower final pH and through a successive addition of the reactants (sample 2), the TPR profile significantly changes. Although a two-step profile is still observed, the intensity of the first peak (shoulder) is now occurring in the same temperature range (around 310 °C) as that reflecting the reduction of the very small CuO islets exhibited by sample 1 (Fig. 5). Its intensity is smaller than that of the similar peak related to the reduction of 30–35 nm sized CuO clusters in sample 1, which well reflects the reduction of (a decreased amount of) large (about 60 nm) CuO clusters in sample 2. As discussed previously [19], the shift of the TPR peak towards higher temperatures (310 °C instead of 262 °C in sample 1) can reflect a slower diffusion of hydrogen through larger clusters and thus their slightly retarded reduction.

The second peak logically accounts for the further reduction of the sub-nanometric CuO islets. It is more intense than in sample 1 because their amount has increased. It also occurs at a higher temperature (342 °C instead of about 320 °C), suggesting a slightly stronger CuO-support interaction (more difficult reduction) than in sample 1.

It is interesting to note that the larger the number of the sub-nanometric particles, the stronger their apparent interaction with the support (TPR) independently on their actual (small) size (not directly observed). In other words, a better dispersion of the CuHN precursors induced by slight pH changes would favor their more efficient attachment to the support and, logically, their more efficient scraping away during thermal accretion, resulting in numerous small but strongly attached CuO particles. Note that TPR data only provide indications about the retention of the CuO precursors while the interaction of the resulting reduced species (here Cu_2O) cannot be directly evaluated by that technique.

Without surprise, a very similar two-step reduction is also observed for sample 3, prepared at the same pH through the simultaneous addition of the reactants (Fig. 5). The first shoulder, still appearing around 310 °C, is related, as for sample 2, to the presence of large CuO clusters within the mesoporous alumina phase. Their size distribution (histogram in Fig. 4b) argues for a population involving, on the average, a mean size of 20–25 nm, thus smaller than that measured for sample 2

and even smaller than that measured for sample 1, which apparently contradicts the attribution of the TPR intensities.

The histogram of sample 3 also shows that a significant amount of CuO particles involve quite large sizes, extending up to 70 nm, in contrast to sample 1 in which the largest CuO particles do not overstep 50 nm. To estimate the influence of the amount of Cu involved in the largest particles of sample 3 on the whole TPR profile, we have evaluated, for both samples 1 and 3 (the two samples for which we could build histograms), the total amount of copper that is reducible in a particle having a given size, a property that is more readily related to the intensity of the TPR peaks than the number of particles having a given size. Each particle being arbitrary assumed to be spherical, from their relative numbers (histograms), it was possible to compute their total volume, that is normally proportional to the amount of Cu in each particle. By arbitrary considering that particles smaller than 40 nm would give rise to a TPR peak occurring around 260 °C (as in sample 1), we have evaluated the % of Cu involved in such particles for both samples 1 and 3. It was found that while 80% of copper is located in particles of less than 40 nm in sample 1, only 44% of Cu belongs to similar sized particles in sample 3. This trend indicates that most of the copper (56%) is located in particles bigger than 40 nm in sample 3, which explains their retarded reduction (TPR main peak found only at about 310 °C, Fig. 5) due to a slower hydrogen diffusion. Actually, in sample 3, the hydrogen consumption that starts to be detected before 200 °C and that extends as a shoulder up to 270 °C before the main peak is recorded (Fig. 5), accounts reasonably well for the reduction of the first 44% of copper located in particles smaller than 40 nm.

The second intense peak was found at almost the same temperature (about 358 °C instead of 342 °C for sample 2), suggesting an equivalent or a slightly stronger retention of the very small CuO particles on the alumina support.

TPR profiles of the two samples prepared by impregnation are shown in Fig. 6 and compared with their analogous Cu–Al_2O_3 mesoporous phase (sample 1). Sample 4 (Cu-impregnated mesoporous alumina) is characterized by a single strong reduction peak with a maximum at 334 °C (Table 3). Compared to sample 1, calcined sample 4 is still "clean" from any CuO cluster (TEM) and, as discussed above, probably involves a spinel-like superficial composition. The

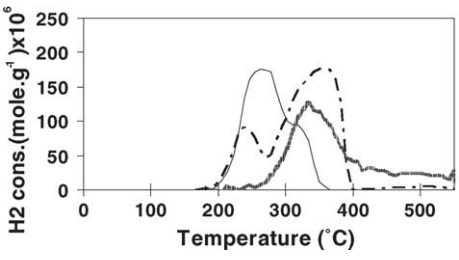

Fig. 6. TPR profiles (Table 3) of two impregnated CuO-Al_2O_3 samples: sample 4 (bold gray curve) and sample 5 (discontinuous curve), compared to a CuO-Al_2O_3 mesoporous phase, sample 1 (full curve).

reduction of such a phase occurs at a fairly low temperature with respect to bulky $CuAl_2O_4$ (T_{red} above 450 °C) but this is not surprising owing to the extremely thin wall structure of the mesophase. The hydrogen consumption indicates a mean oxidation state of copper close to 1 in the reduced residue while no further Cu or Cu_2O clusters are visible on the TEM image. The final reduced Cu phase is therefore expected to still belong to the alumina framework. They at least do not constitute anymore isolated superficial Cu_2O clusters as in samples 1–3. This is obviously inherent to the preparation methods of both sets of samples. Only the direct synthesis yields superficial CuHN islands that stay at the surface after calcination (as CuO clusters) and reduction (as Cu_2O clusters), readily available as catalytic centers. Oppositely, in sample 4, one should expect that the reduced Cu species are "diluted" within the matrix, probably still available as superficial catalytic centers (influencing favorably the activity) but in a different electronic state than in sample 1 (questionable for selectivity).

By contrast, the TPR profile of the classical impregnated Cu/Al_2O_3 is markedly different. The reduction of sample 5 proceeds in two distinct steps (Fig. 6, Table 3). The first TPR peak of medium intensity starts to appear at 150 °C with a maximum at 230 °C while another more important reduction wave shows up at 360 °C and is almost achieved at 400 °C. These two TPR peaks reflect a bimodal size distribution of the resulting metallic copper particles, stemming from the reduction of the corresponding CuO clusters, confirming the data obtained from the TEM analysis. The first peak appearing at 250 °C corresponds to the reduction of medium sized CuO particles, yielding metallic copper particles of 20–30 nm. The second broader peak at 360 °C is evidently due to the reduction of the very large CuO aggregates (>1000 nm). Their bulky size (representing about 80% of the total CuO amount, as suggested by the relative intensities of both TPR peaks) would slow down the diffusion of hydrogen through the particles, and thereby retard their reduction, as already observed in samples 2 and 3 (see above), for other similar Cu mesophases [19] and currently reported in the literature for other systems [24–25].

3.4. Hydrogenation of cinnamaldehyde in liquid phase

The reaction pathway for cinnamaldehyde hydrogenation is shown in Fig. 7. Cinnamaldehyde conversion as a function of time on stream over the three binary mesoporous samples prepared by direct synthesis is reported in Fig. 8a.

The CNA conversion rates for samples 1–3 (Table 4) follow the same trend for the whole series. In fact, they are almost identical for the two samples synthesized at pH = 6.1 (samples 2 and 3), while that of sample 1 is a little bit higher. This suggests that the three compounds roughly exhibit the same surface of the reduced Cu species available for the catalytic act. The unusually high selectivity towards the unsaturated alcohol (CNOL) exhibited by all the binary mesoporous Cu–Al phases prepared through direct synthesis (Fig. 8b and

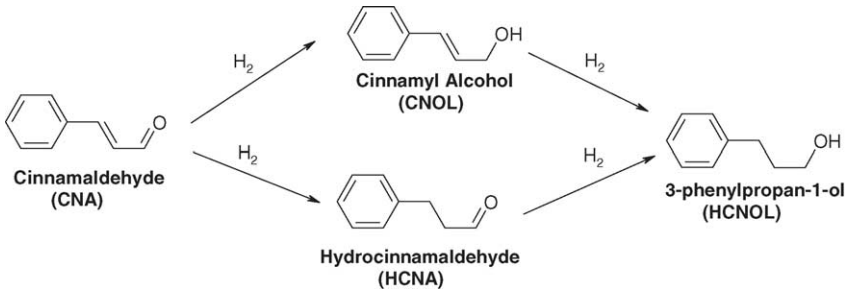

Fig. 7. Reaction scheme for cinnamaldehyde hydrogenation.

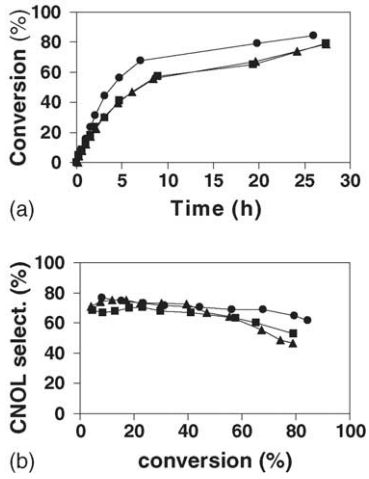

Fig. 8. (a) Cinnamaldehyde conversion as a function of time on stream and (b) CNOL selectivity vs. conversion, over three binary Cu-Al_2O_3 mesoporous samples prepared by direct synthesis: (●) sample 1, (▲) sample 2, (■) sample 3.

Table 4), could be exclusively due to the very small Cu_2O islets that are homogeneously dispersed throughout the alumina matrix. Because the sub nanometric Cu_2O particles stay more homogeneously dispersed onto the surface of the mesoporous alumina phase than the larger Cu^0 clusters (both species being active in hydrogenation [13]), they would favor more readily the hydrogenation of the electro-accepting end of the cinnamaldehyde molecule, namely the carbonyl group, resulting in a high CNOL selectivity. The Cu_2O particles dispersed at the interface of the alumina sheets are more easily available for a direct interaction with the carbonyl group of the bulky cinnamaldehyde molecule, owing to their very small size. Oppositely, for larger Cu^0 particles, a lower CNOL selectivity is observed, as expected. The (electro-donating) C=C bond is therefore more readily hydrogenated on these clusters that are in weaker interaction with the support, as it was observed on classical Cu-impregnated alumina catalysts in this work (see below) and in the literature [14].

Moreover, the fact that all the reduced mesoporous Cu–Al phases exhibit an analogous selectivity towards the unsaturated alcohol confirms that the simultaneous addition of all the reactants during the synthesis is not a required condition to generate performant and very selective hydrogenation catalysts. An appropriate pH adjusting is perhaps more important to obtain phases with optimal mesoporosity and a consequent desired copper dispersion and stabilization. A successive addition of the reactants, far easier to handle, should therefore be privileged for a potential industrial transposition of the synthesis protocol.

The catalytic performances (activity and CNOL selectivity) of the two Cu-impregnated mesoporous and commercial alumina supports have also been evaluated (samples 4 and 5) and compared to the corresponding binary mesoporous phase prepared through direct synthesis (sample 1). In line with what was generally observed in the case of Cu^0 supported on various oxides [26], the activity of each of the two impregnated catalysts should be proportional to the total superficial Cu^0 available, which depends, in the present case, only on the average particle size (the total amount of Cu in each sample is the same). Sample 4 shows the highest activity per g of Cu (Fig. 9a, Table 4), which is easily explained by the favorable surface to volume ratio involved in the very small atomically dispersed reduced copper species. By contrast, sample 5, that mainly exhibits large bulky copper aggregates, is far less active (Fig. 9a), due to the very low dispersion of Cu^0 particles on the support.

Table 4
Catalytic results of the various Cu-Al mesoporous and impregnated samples for cinnamaldehyde hydrogenation in liquid phase

Sample (precursor)	V_i (mol h^{-1} g^{-1})× 10^3	Selectivity (%)		
		HCNA	HCNOL	CNOL
1. Cu-Al meso (pH = 6.5, simultaneous)	5.60	23.0	6.8	70.2
2. Cu-Al meso (pH = 6.1, adjustment)	3.90	22.0	11.9	66.0
3. Cu-Al meso (pH = 6.1, simultaneous)	4.55	23.4	11.3	65.3
4. $Cu_{impregnation}/Al_2O_3$ mesoporous	17.82	69.1	8.4	22.6
5. $Cu_{impregnation}/Al_2O_3$ commercial	5.03	59.3	12.4	28.3

All selectivities were compared at 50% conversion.

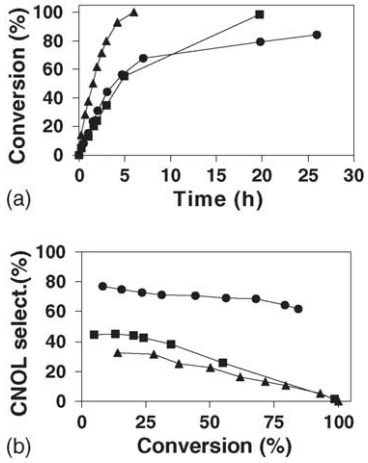

Fig. 9. (a) Cinnamaldehyde conversion as a function of time on stream and (b) CNOL selectivity vs. conversion, over two impregnated Cu-Al_2O_3 samples (▲, sample 4; ■, sample 5) compared to a Cu-Al_2O_3 mesoporous phase (●, sample 1).

Independently on the dispersion state of impregnated copper in both samples, the CNOL selectivity is similar and markedly lower (<30% at 50% conversion) in comparison to that observed with sample 1 generated through direct synthesis (70.2% selectivity). This indicates that the electronic states of the various supported reduced Cu particles in the two samples are probably similar and certainly completely different from those generated on samples prepared by direct synthesis. While in the case of γ-alumina, a weak metal-support interaction after subsequent calcination and reduction steps is expected, nothing can be predicted for the reduced "copper aluminate" type phase (sample 4). Apparently, the electronic state of these latter copper species, although probably different from that of Cu^0 clusters in sample 5, is still not appropriate for an optimum selectivity in hydrogenating the carbonyl bond of the bulky aldehyde. Both systems show a "classical" ∼30% selectivity, as regularly reported in the literature for many such catalysts involving Cu^0 or Cu(I) species supported on various substrates [13,16,27]. These metallic particles in weak interaction with the support, but also the reduced copper species dispersed within a spinel-type framework, would behave as electro-acceptors towards the cinnamaldehyde molecule and would therefore more readily interact with the electro-donor part of the CNA molecule (the conjugated C–C bond), preferentially leading to the hydrocinnamaldehyde (saturated aldehyde).

All these results definitively confirm that our direct synthesis procedure leads to the formation of binary Cu–Al mesoporous phases that exhibit, after calcination and further reduction, extremely promising catalytic performances in selective hydrogenation.

4. Conclusion

A series of binary Cu–Al mesoporous phases prepared by varying some parameters during their one-step synthesis proved excellent catalysts in selective hydrogenation of conjugated unsaturated carbonyl compounds. They are not only active but also particularly selective in the hydrogenation of the carbonyl group of cinnamaldehyde, at the expense of the conjugated C–C double bond. This is due to the presence of a large number of nanometer sized Cu_2O particles, well dispersed and probably in strong interaction with the mesoporous alumina walls. This crucial situation originates from a couple of mechanisms that govern the formation of the mixed mesoporous phases. First, the as-synthesized Cu–Al mesophase prepared at pH around 6.5 ends up with a mesoporous ripple sheeted alumina homogeneously studded with regularly dispersed Cu^{2+} hydroxynitrate islands. After calcination, combined TEM and EDX analyses revealed in all the Cu–Al mesoporous samples, the presence of both (sub)nanometer sized CuO islands and of larger CuO areas, both relatively homogeneously dispersed. An original accretion model could reflect their steady formation upon heating. We have shown that the size of these particles critically depends on a few synthesis variables within the general conditions used. For example, while the sample synthesized at pH 6.5 exhibits many 30–35 nm sized CuO domains, the sample prepared under similar conditions but at pH 6.1, reveals an increased amount of very small CuO islets associated with a lower amount of 25 nm sized CuO particles. By adding the surfactant and basic solutions successively and not simultaneously, at same pH, an even more important amount of (sub)nanometer sized CuO particles coupled to the formation of very few larger and aggregated CuO particles is instantaneously generated. Upon further reduction, all these CuO areas respectively yield sub-nanometric Cu_2O particles, and larger Cu^0 particles that keep a relatively uniform size. The particular conditions used in our one-step preparation are exclusively required for a homogeneous dispersion of both types of particles on the substrate that could be monitored by a careful selection of specific synthesis parameters, such as the final pH of the medium. The dual small size and excellent dispersion of the sub-nanometric particles are the key properties to control for the efficient use of such systems as highly selective catalysts in hydrogenation reactions.

In contrast to the case of classical Cu-impregnated commercial γ-alumina sample that exhibits a very heterogeneous distribution of large CuO aggregates, the Cu-impregnated mesoporous alumina, when calcined, surprisingly only displays very small sub-nanometer sized CuO particles. However, despite these Cu spots are highly dispersed within the mesoporous alumina surface, possibly upon the consequent formation of a mesoporous Cu aluminate type phase upon heating at a moderate temperature, these atomically dispersed species, when reduced, are poorly selective in the transformation of cinnamaldehyde to cinnamyl alcohol. This underlines the need to generate Cu_2O or Cu^0 particles that are not only well dispersed but that belong to separate domains in close interaction with the support but not forming with it a defined phase.

Acknowledgement

The authors gratefully acknowledge Mr Stéphane Pronier (Service de Mesures Physiques de l'UMR 6503 de l'Université de Poitiers) for recording combined TEM-EDX analyses and for constructive discussions.

References

[1] G. Centi, S. Perathoner, Appl. Catal. A 132 (1995) 179.
[2] A. Alejandre, F. Medina, P. Salagre, J.E. Sueiras, Appl. Catal. B 16 (1998) 53.
[3] K. Klier, Adv. Catal. 31 (1981) 243.
[4] J.L.G. Fierro, in: Proceedings of the 8e Seminario Brasileiro de Catalise, vol. II, IBP (Ed.), Rio de Janeiro, Brazil, 1995, p. 544.
[5] M. Englisch, A. Jentys, J.A. Lercher, J. Catal. 166 (1997) 25.
[6] R.L. Augustine, L. Meng, Proceedings of the 16th Conference on Catalysis of Organic Reactions, The Organic Reactions Catalysis Society, Atlanta, GA, USA, 1996.
[7] P. Kluson, L. Cerveny, Appl. Catal. A 128 (1995) 13.
[8] W. Yu, Y. Wang, H. Liu, W. Zeng, J. Mol. Catal. A 112 (1996) 105.
[9] D.V. Sokokskii, N.V. Anisimova, A.K. Zharmagambetova, S.G. Mukhamedzhanova, L.N. Edygenova, React. Kinet. Catal. Lett. 33 (1987) 399.
[10] S. Galvagno, A. Donato, G. Neri, R. Pietropaolo, D. Pietropaolo, J. Mol. Catal. 49 (1989) 223.
[11] S. Galvagno, C. Capannelli, G. Neri, A. Donato, R. Pietropaolo, J. Mol. Catal. 64 (1991) 237.
[12] F. Coloma, A. Sepúlveda-Escribano, J.L.G. Fierro, F. Rodriguez-Reinoso, Appl. Catal. A 148 (1996) 63.
[13] J. Jenck, J.E. Germain, J. Catal. 65 (1980) 141.
[14] A. Chambers, S.D. Jackson, D. Stirling, G. Webb, J. Catal. 168 (1997) 301.
[15] J.C. Rodriguez, A.J. Marchi, A. Borgna, A. Monzón, J. Catal. 171 (1997) 268.
[16] A.J. Marchi, D.A. Gordo, A.F. Trasarti, C.R. Apesteguía, Appl. Catal. A 249 (2003) 53.
[17] S. Valange, J.L. Guth, F. Kolenda, S. Lacombe, Z. Gabelica, Micropor. Mesopor. Mater. 35/36 (2000) 597.
[18] S. Valange, Z. Gabelica, Mesoporous Molecular Sieves, in: L. Bonneviot, F. Béland, C. Danumah, S. Giasson, S. Kaliaguine (Eds.), Studies in Surface Science and Catalysis, vol. 117, 1998, p. 95.
[19] S. Valange, J. Barrault, A. Derouault, Z. Gabelica, Micropor. Mesopor. Mater. 44/45 (2001) 211.
[20] S. Valange, Z. Gabelica, J.M. Clacens, A. Derouault, J. Barrault, in: M.M.J. Treacy, B.K. Marcus, M.E. Bisher, J.B. Higgings (Eds.), Proceedings of the 12th International Zeolite Conference, Baltimore 1998, MRS, Warrendale, PA, USA, 1999, p. 651.
[21] E.P. Barrett, L.G. Joyner, P.H. Halenda, J. Am. Chem. Soc. 73 (1951) 373.
[22] A.F. Wells, Structural Inorganic Chemistry, 5th ed., Clarendon Press, Oxford, 1984.
[23] A. Wolberg, J.F. Roth, J. Catal. 18 (1969) 250.
[24] A. Jones, B.D. McNicol, Temperature Programmed Reduction for Solid Materials Characterization, Marcel Dekker, New York, 1986.
[25] M. Hartmann, S. Racouchot, C. Bischof, Micropor. Mesopor. Mater. 27 (1999) 309.
[26] K.C. Waugh, Catal. Lett. 58 (1999) 163.
[27] R. Hubaut, J.P. Bonnelle, M. Daage, J. Mol. Catal. 55 (1989) 170.